Applied Water Science (2020) 10:243
https://doi.org/10.1007/s13201-020-01326-9

ORIGINAL ARTICLE

Aquatic plant, *Ipomoea aquatica*, as a potential low-cost adsorbent for the effective removal of toxic methyl violet 2B dye

Tze Ling Kua[1] · Muhammad Raziq Rahimi Kooh[2] · Muhammad Khairud Dahri[1] · Nur Afiqah Hazirah Mohamad Zaidi[1] · YieChen Lu[1] · Linda Biaw Leng Lim[1]

Received: 6 September 2019 / Accepted: 28 October 2020 / Published online: 22 November 2020

Abstract

Ipomoea aquatica (IA) was investigated for its potential as a low-cost adsorbent to remove toxic methyl violet 2B (MV2B) dye in aqueous solutions. Optimising parameters such as the effects of contact time, medium pH and ionic strength (using NaCl, $NaNO_3$, KCl and KNO_3) were investigated. The results indicated that 150 min were sufficient for the adsorption to reach an equilibrium state and no adjustment of pH medium was necessary. Batch adsorption experiments such as adsorption isotherm, thermodynamics and kinetics were investigated and the experimental isotherm data were fitted to six isotherm models, namely Langmuir, Freundlich, Temkin, Dubinin-Radushkevich, Redlich-Peterson and Sips, with the latter being the best-fit isotherm model showing maximum adsorption capacity (q_{max}) of 267.9 mg g^{-1}. Thermodynamics studies indicated adsorption of MV2B to be exothermic in nature, occurring spontaneously. The kinetics was best described by the pseudo-second-order model. Regeneration of IA pointed to its reusability, maintaining high adsorption capacity even up until Cycle 5 when treated with acid (HCl) and base (NaOH). Functional groups such as hydroxyl and amine groups which could be involved in the adsorption of MV2B were determined using FTIR spectroscopy, and the point of zero charge of IA was found to be at pH 6.81.

Keywords Water spinach adsorbent · Cationic methyl violet dye · Adsorption isotherm · Kinetics · Thermodynamics · Regeneration

Introduction

Environmental pollution refers to the contamination of the environment due to the introduction of pollutants that can cause harm and damage not only to the environment but also to human and other living organisms. It occurs because the rate of introduction of elements into the nature increases at a rate faster than natural processes can destroy them. Environmental pollution became significant since the industrial revolution in the nineteenth century and has become a major concern to the world today due to its negative effects on human health and environment and is increasing at a fast rate day by day.

One of the major environmental pollutions that cause significant damage to the environment and human health is water pollution. The main causes of water pollution are from industrial activities, agricultural activities and residences as they release harmful and toxic substances such as synthetic dyes and heavy metals into the waterbodies. Since water is a survival necessity to all living organisms including human, water pollution can directly affect our health or even endanger our life. In addition, water pollution also harms aquatic organisms which in turn affects the food chain and also creates water-borne diseases such as diarrhoea, cholera, typhoid fever and malaria.

Since waterbodies are the main reservoirs of water pollutants, wastewater treatment becomes important in addressing the issues of water pollution. Of the many wastewater treatments, adsorption has become the more popular and widely used method to remove pollutants such as dyes in wastewater due to its simplicity in design, low operating cost, high

✉ Linda Biaw Leng Lim
linda.lim@ubd.edu.bn

[1] Chemical Sciences Programme, Faculty of Science, Universiti Brunei Darussalam, Gadong BE1410, Brunei Darussalam

[2] Centre for Advanced Material and Energy Sciences, Universiti Brunei Darussalam, Gadong BE1410, Brunei Darussalam

removal efficiency and flexibility of the adsorption method. In addition, adsorption method often does not produce harmful side-products. Adsorption refers to the enrichment or accumulation of a substance from a liquid phase onto the surface of a solid (Worch 2012). The solid onto which adsorption occurs on the surface is the adsorbent whilst the substance that adsorbs onto the surface of adsorbent is the adsorbate. Many researchers in this field have reported various low-cost adsorbents with high adsorption capability in the removal of dyes in wastewater, some of which are agricultural or industrial solid wastes (Mo et al. 2018; Hussain et al. 2018; Adeniyi and Ighalo 2019; Adeyemo et al. 2017; Bharathi and Ramesh 2013; Kooh et al. 2018).

Synthetic dyes are one of the major organic pollutants that affect waterbodies. They are chemicals that have colouring properties as they attach themselves to the surface of fabrics or other substances to impart colour (Yagub et al. 2014). Synthetic dyes are widely used in textile, food processing, paper and pulp, paint and cosmetics industries for colouring purposes. These industries then discharge the dye wastes into waterbodies which cause water pollution.

In this study, the inedible stems of *Ipomoea aquatica* (IA) was investigated as an adsorbate for the removal of a dye in aqueous solutions by adsorption method because being inedible, the stems are usually thrown away. IA, a semi-aquatic tropical plant that grows well on moist soil or in water, belongs to the family of *Convolculaceae* or morning glory and is commonly found in the tropical or subtropical regions around the world. It is a fast-growing and perennial or annual plant that grows in a creeping or sprawling manner. The stems are 2–3 m long and they usually spread over the ground, on surface of water or intertwine with other plants for support. IA is commonly known as water spinach in general, and as "*kangkong*" in Southeast Asian countries. It is a popular leafy vegetable where the young leaves and shoots are used as an ingredient in Southeast Asian dishes. In Brunei Darussalam, it is often stir-fry with spicy *sambal belacan* (fermented shrimp paste) sauce. Apart from being used in culinary dishes, IA is also an herbaceous plant where the leaf extracts are used to treat jaundice and nervous debility whilst the juice is used for nosebleed and high blood pressure (Prasad et al. 2008).

Methyl violet 2B (MV2B), an adsorbate investigated in this study whose structure, is shown in Fig. 1 and is also known as Basic violet 1. MV2B is a cationic dye and is soluble in water giving a deep violet colour, although the colour of MV2B in solid powder form is dark green. It is often used as a colouring dye for textiles, inks and paints. In addition, MV2B is an active ingredient present in Gram's biological stain which is used for bacterial classification (Conn 1940). MV2B was reported to cause inhibition on the growth of bacteria and photosynthesis of aquatic plants (Kooh et al. 2016). Furthermore, MV2B is also a potential carcinogen

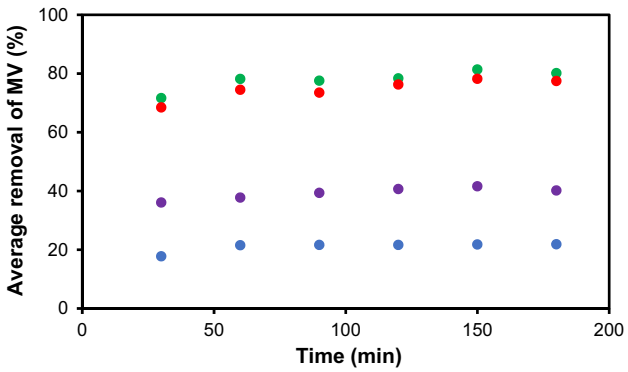

Fig. 1 The effect of contact time on adsorption MV2B on IA at different dye concentrations [50 mg L^{-1} (●), 100 mg L^{-1} (●), 200 mg L^{-1} (●) and 500 mg L^{-1} (●)]

and can cause severe irritations to the eye, skin and respiratory tracts in human (Vachalkova et al. 1996). Due to these harmful effects of MV2B, its removal from waterbodies is important. To date and to the best of our knowledge, there has only been one report on the use of IA as an adsorbent in the removal of Auramine O dye (Lu et al. 2020). Being fast-growing in nature, IA is readily available in abundance and therefore a potentially good low-cost adsorbent.

Hence, this study aims to evaluate IA as a potential low-cost adsorbent towards the removal of MV2B dye. Important parameters such as the time required for the IA-MV2B system to reach equilibrium, the effects of pH and presence of salts on the adsorption of dye will be studied. Investigation of the adsorption characteristics of IA will also be carried out and the data obtained from adsorption isotherm and kinetics will be fitted to various models in order to help provide insight into the adsorption process. Regeneration studies will also be performed in order to determine if it is feasible for IA to be regenerated and reused.

Materials and methods

Chemicals and reagents

MV2B ($C_{24}H_{28}N_3Cl$, 393.959 g mol^{-1}), sodium phosphate monobasic dihydrate (BioUltra grade, ≥99% purity), NaCl (BioXtra grade, ≥99.5% purity) and $NaNO_3$ (ACS grade, ≥99% purity) were purchased from Sigma-Aldrich Chemical Company. HCl, KNO_3 and NaOH were purchased from Merck. KCl (≥99.5% purity) was purchased from May & Baker Ltd. Distilled water was used in the preparation of all stock solutions and throughout all experiments. The stock solution of 1000 mg L^{-1} MV2B was prepared by dissolving accurate amount of MV2B in distilled water, and the other concentrations of MV2B were prepared by diluting

the MV2B stock solution. All adjustments of pH were done using 0.1 M NaOH and 0.1 M HCl solutions. All chemicals and reagents were used as received and without any further purification.

Preparation of the adsorbent

IA was purchased from local vegetable markets and supermarkets. The edible parts were picked whilst the leftover inedible stems were used as the adsorbent in this investigation. The stems were first washed and cleaned thoroughly with running tap water numerous times to remove all soils and dirt and then washed with distilled water. After washing, the cleaned stems were spread out on paper towels and air-dried to evaporate off surface water which will quicken the drying process in the oven. The stems were then dried in the Memmert oven at 65 °C for 3 days until a constant mass was obtained. The dried stems were blended using the Panasonic MX-GM1001 dry mill and sieved through a 355-µm laboratory stainless steel test sieve to obtain powdered IA of particle size <355 µm. This was used as the adsorbent throughout all experiments in this investigation. The powdered IA was stored in an air-tight glass bottle to prevent oxidation and contamination.

Adsorption experiments

MV2B dye stock solution of 1000 mg L^{-1} was prepared, and the solution was sonicated to ensure proper dissolution of MV2B in the distilled water. In all the batch adsorption experiments, the ratio of adsorbent: dye was kept at 1:500 (mass:volume). All adsorbent-dye solution mixtures were shaken using the Stuart SSL1 orbital shakers set at 250 rpm at room temperature for the shaking time determined from the effect of contact time experiment, unless otherwise stated. After shaking, the solutions were filtered through a metal sieve into clean labelled glass vials. The absorbance of diluted filtrates throughout all experiments was measured using the Thermo Scientific Genesys 20 UV-Visible spectrophotometer at 584 nm which is the maximum absorbance wavelength of MV2B. All experiments were performed in duplicates.

The optimising parameters were carried out for contact time (30–180 min), medium pH (pH 2–10) and ionic strength (0–1.0 mol dm^{-3}) using NaCl, $NaNO_3$, KCl and KNO_3. The desired medium pH was adjusted using 0.1 M NaOH and 0.1 M HCl, and measurement of pH was done using the EDT instruments GP353 ATC pH meter.

The batch adsorption isotherm experiments were carried out using MV2B dye concentrations ranging from 0 to 1000 mg L^{-1}. Thermodynamics studies were investigated at 298–343 K and 50, 100, 200 and 500 mg L^{-1} MV2B were used for kinetics studies.

Regeneration of spent adsorbent

Regeneration study was carried out on IA following the method as outlined by Dahri et al. (2015), but using HCl instead of HNO_3. A total of five consecutive cycles were carried out. The dye-loaded IA were treated using four different methods, namely 0.1 M HCl, 0.1 M NaOH, washing with distilled water and quick rinse with distilled water. An untreated spent adsorbent experiment was also carried out as control for comparison purposes.

Point of zero charge

The IA adsorbent (0.05 g) was weighed accurately into ten 150-mL Erlenmeyer flasks, and each flask was labelled properly. 0.1 M KNO_3 solution (25.0 mL) at desired initial pH was added to each flask and was shaken for the optimum contact time. The desired initial pH were pH 2, 4, 6, 8 and 10 which were adjusted using 0.1 M NaOH and 0.1 M HCl. The solutions were shaken for 24 h at 250 rpm at room temperature using an orbital shaker. After shaking, the solutions were filtered through a metal sieve into clean labelled glass vials and the pH of each filtrate was measured using a pH meter. The change in pH was calculated and a graph of change in pH against initial pH was plotted to determine point of zero charge (pH_{pzc}).

Scanning electron microscope analysis

A small amount of IA, before and after adsorption of MV2B, was collected and dried in the oven at 65 °C overnight and then analysed using the JSM-7610F field emission scanning electron microscope (SEM) to determine the surface morphology of the adsorbents.

Fourier transform infrared (FTIR) spectroscopy

A small amount of IA, before and after adsorption of MV2B, was collected and dried in the oven at 65 °C overnight and then analysed using the Agilent Cary 630 FTIR spectrometer in the range of 650–4000 cm^{-1} to determine the functional groups present in the adsorbent which may be responsible for the removal of MV2B.

Results and discussion

Effect of contact time

The effect of contact time is one of the essential optimising parameters to be determined in all adsorption studies as it establishes the optimum contact time for an adsorbent–adsorbate system to reach an equilibrium state. Since

adsorption studies are often applied to wastewater treatment, the determination of contact time is also important in signifying the efficacy and efficiency of an adsorbent in the removal of dyes in wastewater treatment (Lim et al. 2017). In this investigation, the effect of contact time for IA to adsorb MV2B was determined using 50–500 mg L^{-1} dye solutions with shaking time of every 30-min intervals up to 3 h. The results of the effect of contact time are as shown in Fig. 1. As observed, a steep increase in the average percentage removal can be seen in the first 30 min with an average percentage removal of 69% for MV2B. Thereafter, the average percentage removal increased slightly and then slowed down to a plateau at 120 min. The rapid adsorption in the first 30 min is due to the vast availability of vacant active sites on the surface of the adsorbent where adsorption of MV2B occurs (Lim et al. 2015). However, as time progresses, more active sites on the adsorbents became preoccupied with MV2B and the number of vacant active sites became limited. Eventually an observed plateau signifying a saturation point has been reached and the adsorbent–adsorbate system is in an equilibrium state.

Effect of medium pH

In adsorption studies, the effect of medium pH is also one of the important controlling parameters as different medium pH can affect the adsorption of adsorbate on adsorbent by affecting the electrostatic attraction between adsorbate and adsorbent. This is due to and largely depends on the cationic or anionic structure of the adsorbate as well as the surface charge of the adsorbent at that particular medium pH. At the same time, as adsorption is a popular method in wastewater treatment, it is important to determine the effect of different medium pH on the adsorption capacity of an adsorbent as wastewater often contains substances or pollutants that may change the pH of the waterbodies.

The effect of medium pH on the adsorption of 100 mg L^{-1} MV2B on IA in this investigation was limited to within a range of pH 2–10. This is because a report has shown that huge reductions in the colour intensity of MV2B occurred at extreme pH of the medium prior to addition of adsorbent (Kooh et al. 2016). The results of the effect of medium pH are presented in Fig. 2. At pH 2, the average percentage removal of MV2B by IA was 31%, the lowest among the other pH values of the medium. This is because at low acidic pH, large amounts of H^+ ions are present in the medium which compete with the cationic MV2B for the vacant active sites on the surface of the adsorbent (Musyoka et al. 2014). This results in a decrease in the adsorption capacity of the adsorbent. Figure 2 also shows that the average percentage removal of MV2B by IA in medium pH > 4 remained more or less similar at 65–75%. This may be due to a lower amount of H^+ ions present in the medium which decreases

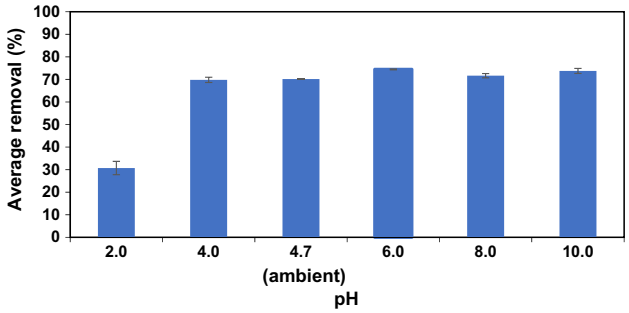

Fig. 2 The effect of medium pH on the adsorption of 100 mg L^{-1} MV2B on IA

the competition of cationic MV2B with H^+ for the active sites. Furthermore, basic condition of the medium can also lead to deprotonation of the functional groups on the adsorbent's surface hence enhancing the electronic attraction between the cationic MV2B and the now anionic surface of the adsorbent. This further increases the adsorption capacity of the adsorbents. As the average percentage removal of MV2B by IA in medium of pH > 4 remained similar with no significant differences compared to the untreated, ambient medium pH of 4.7, the medium pH for all other experiments in this investigation was kept without adjustment of pH for the simplicity and efficiency of the adsorption process.

Effect of ionic strength

The determination of the effect of ionic strength in adsorption studies is another important parameter as wastewater from industries and other sources often contain numerous salts which can influence an adsorbent's adsorption efficiency of dyes in wastewater treatment. Results have shown that the interactions between adsorbent and dye adsorbate were due to electrostatic and hydrophobic interactions (Hu et al. 2013). As discussed previously, a change in medium pH affects the electrostatic interactions between adsorbent and adsorbate. At the same time, a change in the ionic strength of medium can also affect the electrostatic and hydrophobic interactions between adsorbent and adsorbate. An increase in the ionic strength of medium reduces the electrostatic interaction whilst increases the hydrophobic interaction (Dahri et al. 2016).

The effects of ionic strength on the adsorption of 100 mg L^{-1} MV2B on IA using different concentrations of NaCl, $NaNO_3$, KCl and KNO_3 ranging from 0.01 to 1.0 M were determined. The highest percentage removal of MV2B by IA (76%), as shown in Fig. 3, was in the absence of any salts whereby as the concentration of each salt increases, the percentage removal of MV2B by IA generally decreases. The average percentage removal was 60%, 23%, 51% and 46% for 1.0 M NaCl, $NaNO_3$, KCl and KNO_3, respectively.

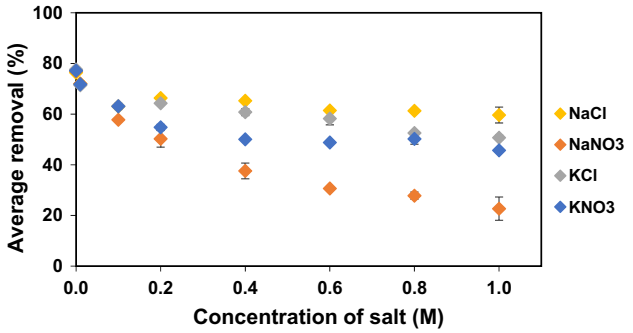

Fig. 3 The effect of ionic strength on the adsorption of 100 mg L^{-1} MV2B on IA using NaCl, $NaNO_3$, KCl and KNO_3 in a concentration range of 0.01–1.0 mg L^{-1}

The reduction in dye removal as the concentration of salts increases (hence ionic strength increases) was due to the presence of positively charged ions such as Na^+ and K^+, which compete with cationic MV2B for the vacant active sites on the surface of adsorbents. In addition, an increase in the ionic strength of the medium causes buildup of cations on the adsorbent's surface which leads to electronic repulsion between the adsorbents and cationic MV2B (Dahri et al. 2015). As a result, the adsorption capacity of the adsorbents decreased. Since the adsorption capacity of IA for removal of MV2B was the highest when no salts were added to the medium, all the other experiments in this investigation were carried out with no addition of any salts.

Adsorption isotherm studies

Adsorption isotherm can be considered the most significant and vital experiment in any adsorption studies as it not only describes the interaction between an adsorbent and adsorbate in an adsorption process but it also provides information regarding the adsorption capacity of an adsorbent for an adsorbate. In this study, six adsorption isotherm models namely Langmuir (Langmuir 1918), Freundlich (Freundlich 1906), Temkin (Temkin and Pyzhev 1940), Dubinin-Radushkevich (D-R) (Dubinin 1947), Redlich-Peterson (R-P) (Redlich and Peterson 1959) and Sips (Sips 1948) were used to describe the adsorption process of MV2B onto IA. Their isotherm equations in nonlinear and linear forms are listed in Table 1.

The Langmuir isotherm model assumes that the maximum adsorption of an adsorbate occurs homogeneously on the surface of an adsorbent resulting in the formation of a saturated monolayer. On the other hand, the Freundlich isotherm model assumes a multilayer adsorption in which the adsorbate can still adsorb on a saturated surface of the adsorbent and that the adsorption occurs heterogeneously on the surface of the adsorbent (Li et al. 2010). The Temkin isotherm model describes the linear decrease in adsorption heat with increasing coverage of the adsorbent's surface as a result of the adsorbent–adsorbate interactions (Li et al. 2010). The D-R isotherm model postulates that the adsorption follows a pore-filling mechanism rather than a layer-by-layer surface coverage mechanism (Hutson and Yang 1997),

Table 1 The nonlinear and linear forms of the six isotherm models

Isotherm model	Nonlinear form	Linear form	Plot
Langmuir	$q_e = \frac{q_{max} K_L C_e}{(1+K_L C_e)}$	$\frac{C_e}{q_e} = \frac{1}{K_L q_{max}} + \frac{C_e}{q_{max}}$	$\frac{C_e}{q_e}$ vs C_e
Freundlich	$q_e = K_F C_e^{1/n}$	$\ln q_e = \frac{1}{n} \ln C_e + \ln K_F$	$\ln q_e$ vs $\ln C_e$
Temkin	$q_e = \frac{RT}{b} \ln K_T C_e$	$q_e = \frac{RT}{b} \ln C_e + \frac{RT}{b} \ln K_T$	q_e vs $\ln C_e$
D-R	$q_e = q_{max} \exp(-\beta\varepsilon^2)$	$\ln q_e = \ln q_{max} - \beta\varepsilon^2$	$\ln q_e$ vs ε^2
	$\varepsilon = RT\left(1 + \frac{1}{C_e}\right)$		
	$E = \frac{1}{\sqrt{2\beta}}$		
R-P	$q_e = \frac{K_R C_e}{1+a_R C_e^{\alpha}}$	$\ln\left(\frac{K_R C_e}{q_e} - 1\right) = \ln a_R + \alpha \ln C_e$	$\ln\left(\frac{K_R C_e}{q_e} - 1\right)$ vs $\ln C_e$
Sips	$q_e = \frac{q_{max} K_S C_e^{1/n}}{1+K_S C_e^{1/n}}$	$\ln\left(\frac{q_e}{q_m - q_e}\right) = \frac{1}{n} \ln C_e + \ln K_S$	$\ln\left(\frac{q_e}{q_m - q_e}\right)$ vs $\ln C_e$

where q_e is amount of adsorbate adsorbed, q_{max} is maximum adsorption capacity, K_L is Langmuir adsorption constant, C_e is the concentration of adsorbate remaining in the solution at equilibrium, K_F is Freundlich constant related to adsorption capacity, n (in Freundlich) is empirical parameter related to adsorption intensity, R is gas constant (8.314 J mol^{-1} K^{-1}), T is absolute temperature (K), b is Temkin isotherm constant, K_T is Temkin isotherm equilibrium binding constant, ε is D-R isotherm constant, E is mean free energy, K_R and a_R are R-P isotherm constants, α is an exponent which lies between 0 and 1, K_S is Sips isotherm constant, $1/n$ is Sips exponent

and this model can generally be applied to adsorption that occurs homogeneously or heterogeneously on the surface of the adsorbent (Chen 2015). The R-P isotherm model is a combination of Langmuir and Freundlich isotherm models which can be applied to homogeneous or heterogeneous systems due to its flexibility. In addition, the R-P isotherm model follows the Freundlich isotherm model at high adsorbate concentration whilst at low adsorbate concentration, it is in accordance with the Langmuir isotherm model (Foo and Hameed 2010). Similar to R-P, the Sips isotherm model is also a combination of Langmuir and Freundlich isotherm models and is used to predict heterogeneous systems. At low adsorbate concentration, the Sips isotherm model assumes the Freundlich isotherm model indicating a multilayer adsorption whilst at high adsorbate concentrate, it assumes the Langmuir isotherm model indicating a monolayer adsorption (Ayawei et al. 2017).

Herein, the best-fit isotherm model for the adsorption of MV2B onto IA is determined based on the highest linear regression coefficient (R^2), lowest error functions and fitting of nonlinear simulated isotherm plots to the experimental isotherm curve. The six error functions in the error analysis of the isotherm models are listed in Table 2.

In this investigation, adsorption isotherm studies on IA were carried out using a range of MV2B concentrations from 10 to 1000 mg L^{-1} under optimised conditions. Using the linear plots from the isotherm equations as shown in Table 1, the isotherm parameters of IA are calculated and presented in Table 3. The linear regression coefficient (R^2) in decreasing order is as follows: Sips > Temkin > D-R > Freundlich > Langmuir > R-P. The invalidity of R-P model in describing the adsorption of MV2B by IA can be further confirmed by its simulation plot, as shown in Fig. 4. Although the D-R model has good R^2 yet its overall error values are the largest and this is further confirmed by the deviation of the D-R simulated isotherm plot in comparison with the respective experimental isotherm curve.

Of the four models left, the Langmuir and Temkin models gave the lowest R^2 and highest error values, respectively, whilst even though the Freundlich model has good R^2, but when compared with the Sips model, the latter has the highest R^2 with the lowest errors. Hence, the Sips isotherm model is chosen as the best fit isotherm model for the adsorption of MV2B on IA, assuming multilayer adsorption onto a heterogeneous surface of IA at low MV2B concentration and monolayer adsorption at high MV2B concentration.

According to the chosen best fit Sips isotherm model, the q_{max} of IA is 267.9 mg g^{-1}, whilst based on the monolayer Langmuir isotherm model is 371 mg g^{-1}. This q_{max} value is considered high compared to other reported adsorbents as shown in Table 4. IA can also serve as a good adsorbent as its production is low cost since it involves oven drying only. Further, its q_{max} value is high when compared to many adsorbents such as orange and banana peel with q_{max} values of 11.5 and 12.2 mg g^{-1}, respectively.

Thermodynamics studies

Apart from room temperature, batch adsorption isotherm studies on the removal of MV2B by IA were also carried out in different temperatures, as shown in Fig. 5a. From the van Hoff's plot in Fig. 5b, the thermodynamics parameters are calculated and presented in Table 5. The negative Gibbs free energy values (ΔG°) suggests that the adsorption process is favourable, whilst the negative enthalpy (ΔH°) suggests that the adsorption process is exothermic in nature. The entropy (ΔS°) is positive which suggests an increase in randomness in the system which may be due to "solvent-replacement"

Table 2 Types of error functions and their expressions

Types of error	Abbreviation	Expression
Average relative error	ARE	$\frac{100}{n}\sum_{i=1}^{n}\left\lvert\frac{q_{e,meas}-q_{e,calc}}{q_{e,meas}}\right\rvert_i$
Sum square error	SSE	$\sum_{i=1}^{n}\left(q_{e,calc}-q_{e,meas}\right)_i^2$
Hybrid fractional error function	HYBRID	$\frac{100}{n-p}\sum_{i=1}^{n}\left[\frac{\left(q_{e,meas}-q_{e,calc}\right)^2}{q_{e,meas}}\right]_i$
Sum of absolute error	EABS	$\sum_{i=1}^{n}\left\lvert q_{e,meas}-q_{e,calc}\right\rvert$
Marquardt's percent standard deviation	MPSD	$100\sqrt{\frac{1}{n-p}\sum_{i=1}^{n}\left(\frac{q_{e,meas}-q_{e,calc}}{q_{e,meas}}\right)_i^2}$
Nonlinear chi-square test	χ^2	$\sum_{i=1}^{n}\frac{\left(q_{e,calc}-q_{e,meas}\right)^2}{q_{e,meas}}$

$q_{e,\,calc}$ and $q_{e,\,meas}$ are calculated and measured adsorption capacity, respectively, n is the number of experimental data points and p is the number of parameters

Table 3 The linear regression coefficients (R^2) and isotherm parameters of Langmuir, Freundlich, Temkin, D-R, R-P and Sips for adsorption of MV2B onto IA

Isotherm model	Values	ARE	SSE	HYBRID	EABS	χ^2
Langmuir		16.95	0.06	1.22	0.68	0.16
q_{max} (mmol g^{-1})	0.94					
q_{max} (mg g^{-1})	371.43					
K_L (L $mmol^{-1}$)	0.0054					
R^2	0.8799					
Freundlich		22.18	0.24	3.53	1.22	0.46
K_F (mmol g^{-1} (L $mmol^{-1})^{1/n}$)	0.0090					
K_F ($mg^{1-1/n}$ $L^{1/n}$ g^{-1})	3.56					
n	1.31					
R^2	0.9111					
Temkin		27.26	0.03	1.41	0.60	0.18
K_T (L $mmol^{-1}$)	0.09					
b (kJ mol^{-1})	13.63					
R^2	0.9568					
D-R		294.50	1.60	155.68	3.94	20.24
q_{max} (mmol g^{-1})	0.58					
q_{max} (mg g^{-1})	228.69					
β ($\times 10^{-6}$ J mol^{-1})	2.99					
E (kJ mol^{-1})	408.89					
R^2	0.9189					
R-P		22.17	0.24	3.82	1.22	0.46
K_R (L g^{-1})	1.00					
α	0.24					
a_R (L $mmol^{-1}$)	110.09					
R^2	0.5035					
Sips		13.00	0.02	0.57	0.41	0.07
q_{max} (mmol g^{-1})	0.68					
q_{max} (mg g^{-1})	267.89					
K_S (L $mmol^{-1}$)	0.0019					
n	0.70					
R^2	0.9747					

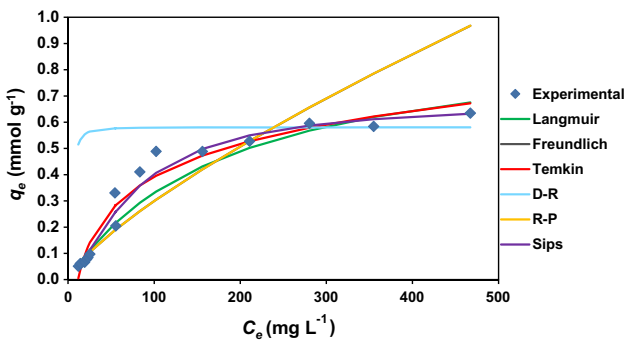

Fig. 4 Simulated isotherm plots of IA in comparison with experimental isotherm curve for adsorption of MV2B

phenomenon, where the water molecules on the surface of the adsorbent needs to be replaced by the MV2B molecules in order to be adsorbed (Ruixia et al. 2004).

Kinetics studies

The study of kinetics in adsorption process is very useful in that it determines the rate of reaction of the system and provides valuable information on the adsorption mechanism (Zehra et al. 2016). In this investigation, two kinetics models were used to describe the adsorbent–adsorbate interactions and to determine the adsorption mechanism and they are the Lagergren's pseudo-first-order kinetics model (Lagergren 1898) and Ho's pseudo-second-order kinetics model (McKay and Ho 1999).

The nonlinear and linear equations of the kinetics models are listed in Table 6. The determination of the best-fit kinetics model is based on the calculated linear regression coefficient (R^2) using linearised kinetics equations, error functions and the closeness in value between calculated q_e from kinetics model and experimental q_e from isotherm. Using the linearised kinetics equations, the parameters and error

Table 4 Comparison table for the adsorption capacity (q_{max}) of different adsorbents for the removal of MV2B

Adsorbent	q_{max} (mg g^{-1})	References
IA (water spinach)	267.9	This work
Orange peel	11.5	Annadurai et al. (2002)
Exfoliated graphene oxide	2.5	Ramesha et al. (2011)
Banana peel	12.2	Annadurai et al. (2002)
Acid-modified activated carbon	83.3	Din and Hameed (2010)
HNT–Fe_3O_4 composite	20.0	Bonetto et al. (2015)
Artocarpus heterophyllus (Jackfruit) seed	126.7	Dahri et al. (2016)
Casuarina equisetifolia Needle	165.0	Dahri et al. (2013)
Azolla pinnata	194.2	Kooh et al. (2015)
Cempedak durian peel	238.5	Dahri et al. (2015)
Furan-2,5-dione-functionalised cellulose	106.4	Musyoka et al. (2014)
Duckweed (*Lemna minor*)	332.5	Lim et al. (2014)
Ghassoul clay	625.0	Elass et al. (2011)
Fe_3O_4 magnetic nanoparticles	416.7	Keyhanian et al. (2016)
Polyacrylamide	1136	Rahchamani et al. (2011)
Artocarpus odoratissimus leaves	139.7	Lim et al. (2016)
A. odoratissimus leaf-based cellulose	187.0	Zaidi et al. (2018)
SDS-modified Fe_3O_4 magnetic nanoparticles	416.7	Keyhanian et al. (2016)
N-benzyltriazole-derivatised dextran	95.2	Cho et al. (2015)
Sulfuric-modified *Saccharum bengalense*	7.3	Din et al. (2017)
Water hyacinth	6.7	Malviya et al. (2017)
Sunflower (*Helianthus annuus* L.) seed hull	92.6	Hameed (2008)
Mesoporous-mixed oxide Ce03Al07	25.0	Phatai and Futalan (2016)

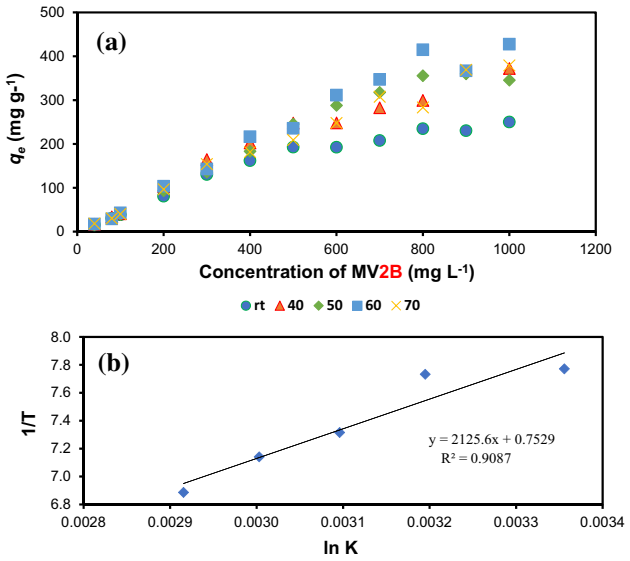

Fig. 5 (**a**) Thermodynamics data of IA at 298–343 K and (**b**) van Hoff's plot

functions of the kinetics models for adsorption of MV2B on IA are calculated and presented in Table 7.

According to Table 7, the R^2 values for IA are the highest and closest to 1 in pseudo-second-order kinetics model for all the concentrations investigated whilst the pseudo-first-order kinetics model has lower R^2 values. Furthermore, the errors from the six error functions (ARE, SSE, HYBRID, EABS, MPSD and χ^2) for IA are the smallest in pseudo-second-order kinetics model. Comparison of the simulation plots of experiment data with the two models in Fig. 6 also shows that the Lagergren pseudo-first-order is not the right model. Hence, based on R^2 and error values as well as comparison of the plots, it can be concluded that the best-fit kinetics model for the adsorption of MV2B onto IA is the pseudo-second-order kinetic model. This is further confirmed by the closeness in values between $q_{e,calc}$ from pseudo-second-order kinetics model and $q_{e,expt}$ from isotherm as tabulated in Table 7.

Regeneration studies

The purpose of regeneration in adsorption studies is to investigate the reusability and capability of a spent adsorbent to adsorb more adsorbate. Regeneration experiment is important and useful in wastewater treatment as an adsorbent with good regeneration capability can help reduce the cost (Dahri et al. 2015). In this investigation, the spent adsorbent (IA) was treated in four ways, namely acid (0.1 M HCl), base (0.1 M NaOH), distilled water and quick rinse with distilled water. A control was also prepared for comparison with the four treatment methods.

Table 5 Thermodynamics parameters for the adsorption of MV2B onto IA

$\Delta H°$ (kJ mol^{-1})	$\Delta S°$ (J mol^{-1} K^{-1})	T (K)				
		298	313	323	333	343
		$\Delta G°$ (kJ mol^{-1})				
−17.67	6.26	−19.26	−20.12	−19.65	−19.77	−19.64
		q_{max} (mg g^{-1})				
		371.4	525.3	597.8	730.3	671.5

Table 6 Nonlinear and linear equations of pseudo-first-order kinetic and pseudo-second-order kinetic models

Kinetics model	Nonlinear equation	Linear equation	Plot
Pseudo-first-order	$q_t = q_e(1 - \exp^{-k_1 t})$	$\log(q_e - q_t) = \log q_e - \frac{k_1}{2.303} t$	$\log(q_e - q_t)$ vs t
Pseudo-second-order	$q_t = \frac{k_2 q_e^2 t}{1 + k_2 q_e t}$	$\frac{t}{q_t} = \frac{1}{k_2 q_e^2} + \frac{t}{q_e}$	$\frac{t}{q_t}$ vs t

where q_t and q_e are amount of dye adsorbed per unit of adsorbent at equilibrium and at time t, and k_1 and k_2 are pseudo-first-order and pseudo-second-order rate constants

Table 7 Parameters and error functions of pseudo-first-order kinetics model and pseudo-second-order kinetics models for adsorption of MV2B on IA

Kinetics model	MV2B (mg L^{-1})			
	50	100	200	500
Pseudo-first-order				
R^2	0.941	0.548	0.884	0.763
$q_{e,calc}$ (mmol g^{-1})	0.019	0.009	0.047	0.246
$q_{e,expt}$ (mmol g^{-1})	0.056	0.098	0.206	0.489
k_1 (min^{-1})	0.034	0.025	0.016	0.023
ARE	39.26	96.76	46.52	98.91
SSE	0.01	0.11	0.29	2.27
HYBRID	1.55	9.30	8.29	41.66
EABS	0.39	1.35	1.78	5.90
MPSD	57.41	103.50	67.73	105.74
χ^2	0.29	1.30	1.58	5.83
Pseudo-second-order				
R^2	0.999	1.000	1.000	0.9964
$q_{e,calc}$ (mmol g^{-1})	0.057	0.092	0.207	0.519
$q_{e,expt}$ (mmol g^{-1})	0.056	0.098	0.206	0.489
k_2 (g mmol^{-1} min$^{-1/2}$)	3.60	10.65	1.40	0.25
ARE	2.76	1.68	1.35	6.93
SSE	0.000	0.001	0.004	0.02
HYBRID	0.02	0.01	0.14	0.41
EABS	0.02	0.02	0.05	0.33
MPSD	6.19	3.76	3.09	12.80
χ^2	0.003	0.002	0.024	0.06

The regeneration experiment proceeded through five consecutive cycles, and the results are presented in Fig. 7. Washing the spent IA with base resulted in the highest percentage removal of 63.7% at Cycle 5 followed by the washing with acid (56.8%). The high percentage removal of spent IA when it is treated with acid and base can be attributed to the acid and base that improved the roughness of the adsorbent's surface and exposed the reactive functional groups on the binding-sites of the adsorbent (Dahri et al. 2015), as NaOH was known to remove natural fats, waxes and low molecular weight lignin (Kooh et al. 2015). On the other hand, the washing of spent IA with distilled water, quick rinse with distilled water as well as the control experiment gave lower percentage removal of 9.0%, 7.3% and 3.43%, respectively, at Cycle 5. However, it must be emphasised that the MV2B concentration used in this study is high (600 mg L^{-1}) when compared to other reported studies. Therefore, IA has good regeneration capability, especially when it is treated with acid or base, and hence has great advantage as an adsorbent in wastewater treatment.

Characterisation of adsorbent

Point of zero charge

The pH_{pzc} of an adsorbent is the pH at which the surface of the adsorbent has a net zero charge. The determination of pH_{pzc} of adsorbents in adsorption studies is an important characterisation as it provides information on how a change in medium pH can affect the adsorption of adsorbate on adsorbent. The value of pH_{pzc} of an adsorbent can determine from the x-intercept of a plot of change in pH (ΔpH) against initial pH of the medium. This is the intercept of the plot where ΔpH is zero. The results from the determination of pH_{pzc} of IA are as shown in Fig. 8 and accordingly, the pH_{pzc} of IA was found to be at pH 6.81. This explains why IA showed a drastic reduction in removal of MV2B at pH 2

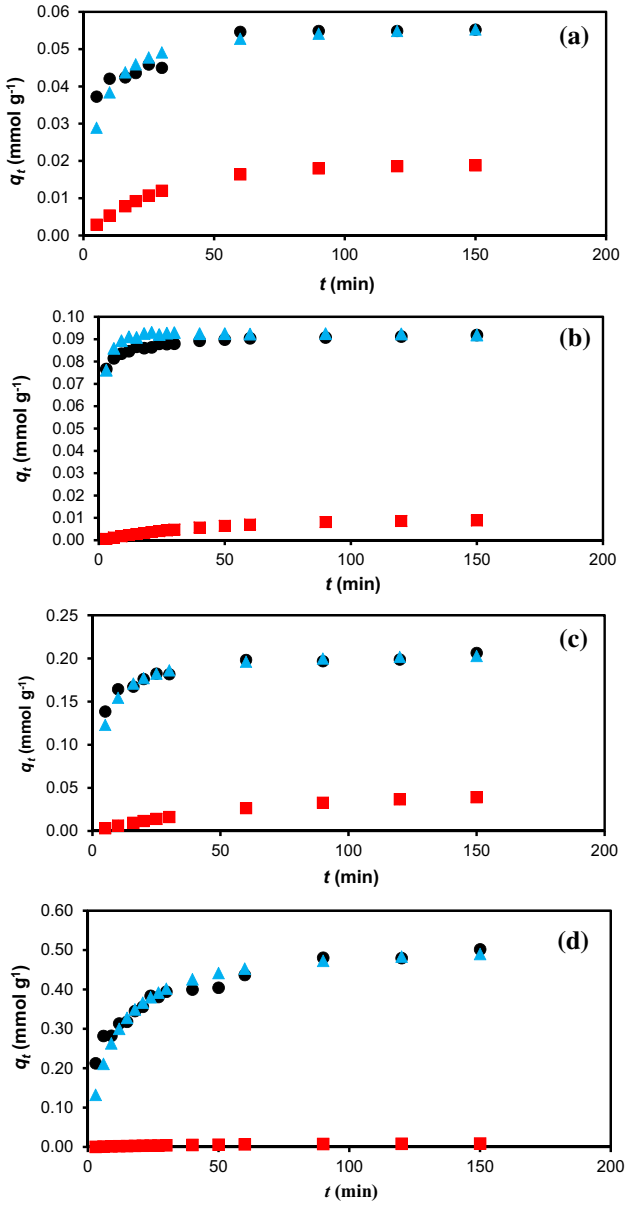

Fig. 6 Comparison of experiment data (●) with the Lagergren pseudo-first-order kinetics (■) and pseudo-second-order (▲) using (**a**) 50 mg L^{-1}, (**b**) 100 mg L^{-1}, (**c**) 200 mg L^{-1} and (**d**) 500 mg L^{-1} MV2B

(Fig. 2). In a medium where pH < pH_{pzc}, functional groups such as carboxyl, hydroxyl and amine present on the surface of adsorbents are protonated due to the availability of large numbers of H^+ ions (Kooh et al. 2016). This causes the surface of the adsorbents to become predominantly positively charged which leads to electronic repulsion between the cationic MV2B and the now positively charged adsorbent (Lim et al. 2015).

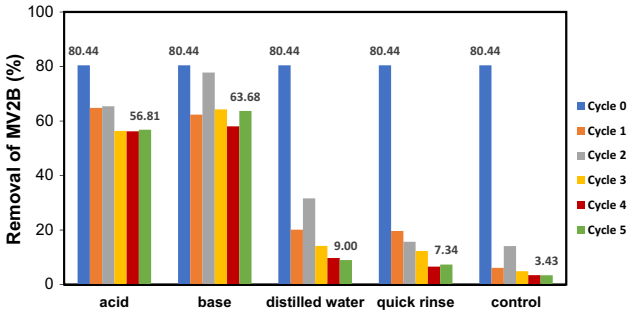

Fig. 7 Regeneration of IA through six consecutive cycles of adsorption using 600 mg L^{-1} MV2B and desorption using acid (0.1 M HCl), base (0.1 M NaOH), distilled water, quick rinse with water and control

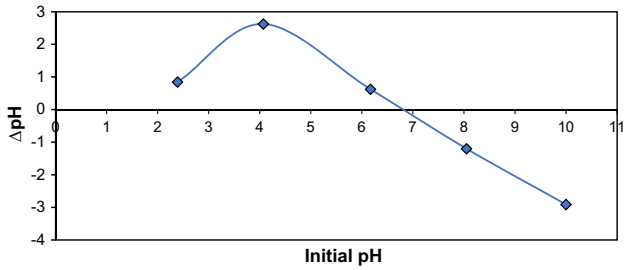

Fig. 8 A linear plot of ΔpH against initial pH of the medium for the determination of pH_{pzc} of IA

SEM analysis

A SEM works by scanning the surface of a solid sample using a focused electron beam to produce a magnified image showing the surface morphology of the sample. The surface morphology of IA, before and after adsorption of MV2B, was analysed using SEM at 500× magnification (Fig. 9). Prior to adsorption of MV2B, the surface of IA appeared to consist of curly fibrous-like strands, rough with many irregular-shaped pores and cavities.

Functional group analysis

FTIR spectroscopy was used to determine the functional groups present in IA which may be responsible for the adsorption process. In this investigation, the FTIR spectroscopy analyses of IA, before and after the adsorption of MV2B, are shown in Fig. 10, and the shifts in the bands were recorded. These shifts could be the functional groups that may be responsible for the adsorption of MV2B on the surface of the adsorbent (Table 8).

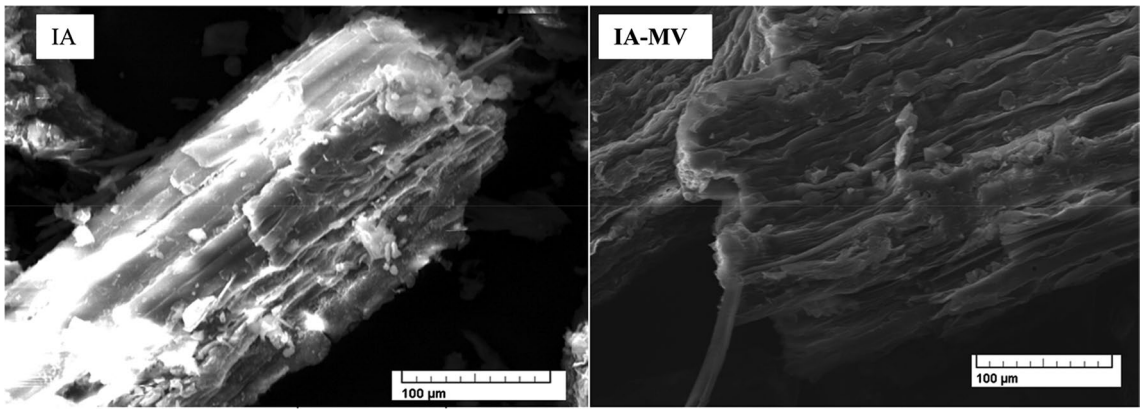

Fig. 9 Scanning electron micrographs of IA before (left) and after (right) adsorption of MV2B at 500× magnification

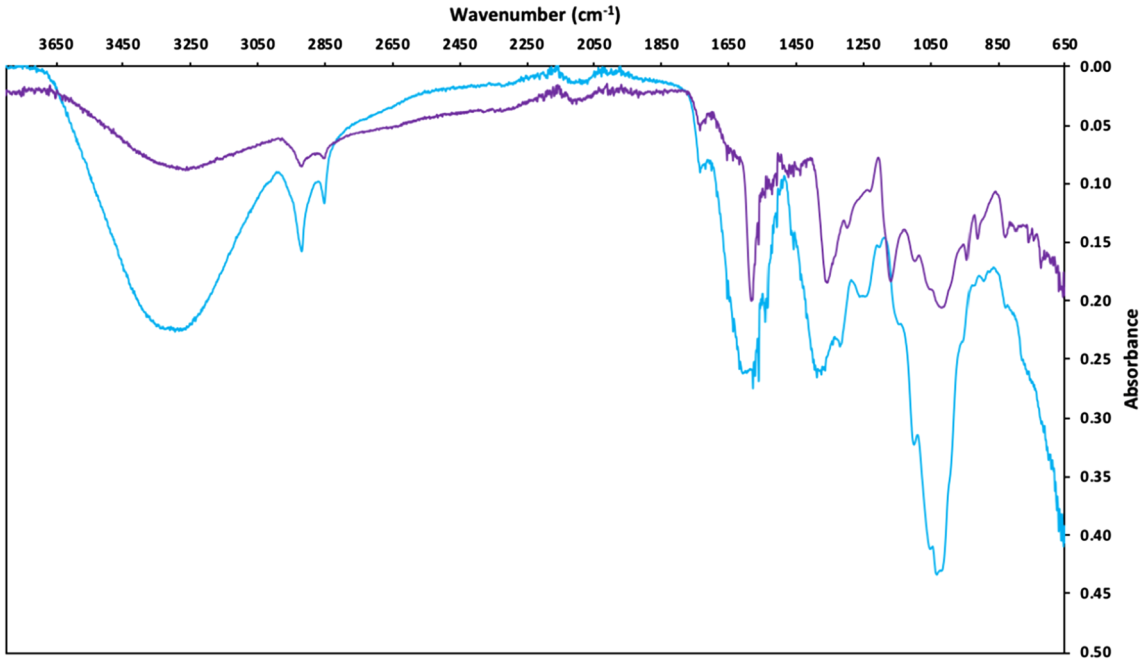

Fig. 10 FTIR spectra of IA before (blue) and after (purple) adsorption of MV2B

Table 8 Shifts in FTIR spectral bands and their responsible functional groups due to adsorption of MV2B on IA

Functional group	Shift in band (cm^{-1})
–OH stretching or –NH stretching	3274–3255
N–H bending	1584–1582
C–O or C–N stretching	1008–1030

Conclusion

In this investigation, IA was successfully used as an adsorbent for the removal of MV2B. The adsorption isotherm of IA was found to be best-fitted to Sips model, giving q_{max} of 267.9 mg g^{-1}, a value higher when compared to many other reported adsorbents. In kinetics studies, the adsorption process obeyed the pseudo-second-order kinetics. Furthermore, IA was investigated for its regeneration ability and was found to be able to maintain high adsorption capacity when treated with acid (HCl) and base (NaOH) even after 5 cycles. Due to the abundance and fast-growing nature of IA with high adsorption capacity and regeneration capability, IA is deemed as a potential low-cost adsorbent in the removal of MV2B in aqueous solutions such as wastewater to alleviate the issues of water pollution.

Acknowledgements Appreciation is given to the Government of Brunei Darussalam and Universiti Brunei Darussalam (UBD) for their offer of Graduate Research Studies scholarship. Appreciation also goes to the Applied Physics and the Environment and Life Sciences Sections of UBD for the usage of the SEM instrument.

Compliance with ethical standards

Funding There is no direct funding to this research study.

Conflict of interest The authors declare that there are no conflicts of interest.

References

Adeniyi AG, Ighalo JO (2019) Biosorption of pollutants by plant leaves: an empirical review. J Environ Chem Eng 7:103100. https://doi.org/10.1016/J.JECE.2019.103100

Adeyemo AA, Adeoye IO, Bello OS (2017) Adsorption of dyes using different types of clay: a review. Appl Water Sci 7:543–568. https://doi.org/10.1007/s13201-015-0322-y

Annadurai G, Juang R-S, Lee D-J (2002) Use of cellulose-based wastes for adsorption of dyes from aqueous solutions. J Hazard Mater 92:263–274. https://doi.org/10.1016/S0304-3894(02)00017-1

Ayawei N, Ebelegi AN, Wankasi D (2017) Modelling and interpretation of adsorption isotherms. J Chem 2017:1–11. https://doi.org/10.1155/2017/3039817

Bharathi KS, Ramesh ST (2013) Removal of dyes using agricultural waste as low-cost adsorbents: a review. Appl Water Sci 3:773–790. https://doi.org/10.1007/s13201-013-0117-y

Bonetto LR, Ferrarini F, de Marco C et al (2015) Removal of methyl violet 2B dye from aqueous solution using a magnetic composite as an adsorbent. J Water Process Eng 6:11–20. https://doi.org/10.1016/J.JWPE.2015.02.006

Chen X (2015) Modeling of experimental adsorption isotherm data. Information 6:14–22. https://doi.org/10.3390/info6010014

Cho E, Tahir MN, Kim H et al (2015) Removal of methyl violet dye by adsorption onto N-benzyltriazole derivatized dextran. RSC Adv 5:34327–34334. https://doi.org/10.1039/C5RA03317A

Conn HJ (1940) Biological stains. A handbook on the nature and uses of the dyes employed in the biological laboratory, 4th edn. Biotech, Geneva, NY

Dahri MK, Kooh MRR, Lim LBL (2013) Removal of methyl violet 2B from aqueous solution using *Casuarina equisetifolia* needle. ISRN Environ Chem 2013:1–8. https://doi.org/10.1155/2013/619819

Dahri MK, Chieng HI, Lim LBL et al (2015) Cempedak durian (artocarpus sp.) peel as a biosorbent for the removal of toxic methyl violet 2B from aqueous solution. Korean Chem Eng Res 53:576–583. https://doi.org/10.9713/kcer.2015.53.5.576

Dahri MK, Kooh MRR, Lim LBL (2016) Adsorption of toxic methyl violet 2B dye from aqueous solution using Artocarpus heterophyllus (Jackfruit) seed as an adsorbent. Am Chem Sci J 15:1–12

Din ATM, Hameed BH (2010) Adsorption of methyl violet dye on acid modified activated carbon: isotherm and thermodynamics. J Appl Sci Environ Sanit 5:151–160

Din MI, Ijaz K, Naseem K (2017) Biosorption potentials of acid modified Saccharum bengalense for removal of methyl violet from aqueous solutions. Chem Ind Chem Eng Q 23:399–409. https://doi.org/10.2298/CICEQ151217054D

Dubinin MM (1947) The equation of the characteristic curve of activated charcoal. Dokl Akad Nauk SSSR 55:327–329

Elass K, Laachach A, Alaoui A, Azzi M (2011) Removal of methyl violet from aqueous solution using a stevensite-rich clay from Morocco. Appl Clay Sci 54:90–96. https://doi.org/10.1016/J.CLAY.2011.07.019

Foo KY, Hameed BH (2010) Insights into the modeling of adsorption isotherm systems. Chem Eng J 156. https://doi.org/10.1016/j.cej.2009.09.013

Freundlich HMF (1906) Over the adsorption in solution. J Phys Chem 57:1100–1107

Hameed BH (2008) Equilibrium and kinetic studies of methyl violet sorption by agricultural waste. J Hazard Mater 154:204–212. https://doi.org/10.1016/J.JHAZMAT.2007.10.010

Hu Y, Guo T, Ye X et al (2013) Dye adsorption by resins: effect of ionic strength on hydrophobic and electrostatic interactions. Chem Eng J 228:392–397. https://doi.org/10.1016/J.CEJ.2013.04.116

Hussain S, Anjali KP, Hassan ST, Dwivedi PB (2018) Waste tea as a novel adsorbent: a review. Appl Water Sci 8:165. https://doi.org/10.1007/s13201-018-0824-5

Hutson ND, Yang RT (1997) Theoretical basis for the Dubinin-Radushkevitch (D-R) adsorption isotherm equation. Adsorption 3:189–195

Keyhanian F, Shariati S, Faraji M, Hesabi M (2016) Magnetite nanoparticles with surface modification for removal of methyl violet from aqueous solutions. Arab J Chem 9:S348–S354. https://doi.org/10.1016/J.ARABJC.2011.04.012

Kooh MRR, Lim LBL, Dahri MK et al (2015) Azolla pinnata: an efficient low cost material for removal of methyl violet 2B by using adsorption method. Waste Biomass Valoriz 6:547–559. https://doi.org/10.1007/s12649-015-9369-0

Kooh MRR, Dahri MK, Lim LBL et al (2016) Batch adsorption studies of the removal of methyl violet 2B by soya bean waste: isotherm, kinetics and artificial neural network modelling. Environ Earth Sci 75:783. https://doi.org/10.1007/s12665-016-5582-9

Kooh MRR, Dahri MK, Lim LBL et al (2018) Separation of acid blue 25 from aqueous solution using water lettuce and agro-wastes by batch adsorption studies. Appl Water Sci 8:61. https://doi.org/10.1007/s13201-018-0714-x

Lagergren S (1898) About the theory of so-called adsorption of soluble substances. K Sven Vetenskapsakad Handl 24:1–39

Langmuir I (1918) The adsorption of gases on plane surfaces of glass, mica and platinum. J Am Chem Soc 40:1361–1403

Li P, Su YJ, Wang Y et al (2010) Bioadsorption of methyl violet from aqueous solution onto Pu-erh tea powder. J Hazard Mater 179:43–48. https://doi.org/10.1016/j.jhazmat.2010.02.054

Lim LBL, Priyantha N, Chan CM et al (2014) Adsorption behavior of methyl violet 2B using duckweed: equilibrium and kinetics studies. Arab J Sci Eng 39:6757–6765. https://doi.org/10.1007/s13369-014-1224-2

Lim LBL, Priyantha N, Mansor NHM (2015) Artocarpus altilis (breadfruit) skin as a potential low-cost biosorbent for the removal of crystal violet dye: equilibrium, thermodynamics

and kinetics studies. Environ Earth Sci 73:3239–3247. https://doi.org/10.1007/s12665-014-3616-8

Lim LBL, Priyantha N, Mohamad Zaidi NAH (2016) A superb modified new adsorbent, Artocarpus odoratissimus leaves, for removal of cationic methyl violet 2B dye. Environ Earth Sci 75. https://doi.org/10.1007/s12665-016-5969-7

Lim LBL, Priyantha N, Tennakoon DTB et al (2017) Breadnut peel as a highly effective low-cost biosorbent for methylene blue: equilibrium, thermodynamic and kinetic studies. Arab J Chem 10:S3216–S3228. https://doi.org/10.1016/J.ARABJC.2013.12.018

Lu YC, Priyantha N, Lim LBL (2020) *Ipomoea aquatica* roots as environmentally friendly and green adsorbent for efficient removal of Auramine O dye. Surf Interfaces 20:100543

Malviya K, Parashar C, Dixit S, Kaur S (2017) Adsorption isotherms and thermodynamics study for methyl violet dye removal from aqueous solution using water hyacinth as an adsorbent. Int J ChemTech Res 10:369–374

McKay G, Ho YS (1999) Pseudo-second order model for sorption processes. Process Biochem 34:451–465

Mo J, Yang Q, Zhang N et al (2018) A review on agro-industrial waste (AIW) derived adsorbents for water and wastewater treatment. J Environ Manag 227:395–405. https://doi.org/10.1016/J.JENVMAN.2018.08.069

Musyoka SM, Mittal H, Mishra SB, Ngila JC (2014) Effect of functionalization on the adsorption capacity of cellulose for the removal of methyl violet. Int J Biol Macromol 65:389–397. https://doi.org/10.1016/J.IJBIOMAC.2014.01.051

Phatai P, Futalan CM (2016) Removal of methyl violet dye by adsorption onto mesoporous mixed oxides of cerium and aluminum. Desalin Water Treat 57:8884–8893. https://doi.org/10.1080/19443994.2015.1027281

Prasad KN, Shivamurthy GR, Aradhya SM (2008) Ipomoea aquatica, an underutilized green leafy vegetable: a review. Int J Bot 4:123–129

Rahchamani J, Mousavi HZ, Behzad M (2011) Adsorption of methyl violet from aqueous solution by polyacrylamide as an adsorbent: isotherm and kinetic studies. Desalination 267:256–260. https://doi.org/10.1016/J.DESAL.2010.09.036

Ramesha GK, Vijaya Kumara A, Muralidhara HB, Sampath S (2011) Graphene and graphene oxide as effective adsorbents toward anionic and cationic dyes. J Colloid Interface Sci 361:270–277. https://doi.org/10.1016/J.JCIS.2011.05.050

Redlich O, Peterson DL (1959) A useful adsorption isotherm. J Phys Chem 63:1024

Ruixia W, Jinlong C, Lianlong C et al (2004) Study of adsorption of lipoic acid on three types of resin. React Funct Polym 59:243–252. https://doi.org/10.1016/j.reactfunctpolym.2004.02.004

Sips R (1948) Combined form of Langmuir and Freundlich equations. J Phys Chem 16:490–495

Temkin MJ, Pyzhev V (1940) Kinetics of ammonia synthesis on promoted iron catalysts. Acta Physiochim 12:217

Vachalkova A, Novotny L, Blesova M (1996) Polarographic reduction of some triphenylmethane dyes and their potential carcinogenic activity. Neoplasma 43:113–117

Worch E (2012) Adsorption technology in water treatment: fundamentals, processes, and modeling. Walter de Gruyter, Berlin

Yagub MT, Sen TK, Afroze S, Ang HM (2014) Dye and its removal from aqueous solution by adsorption: a review. Adv Colloid Interf Sci 209:172–184. https://doi.org/10.1016/j.cis.2014.04.002

Zaidi NAHM, Lim LBL, Usman A (2018) Artocarpus odoratissimus leaf-based cellulose as adsorbent for removal of methyl violet and crystal violet dyes from aqueous solution. Cellulose 25:3037–3049. https://doi.org/10.1007/s10570-018-1762-y

Zehra T, Priyantha N, Lim LBL (2016) Removal of crystal violet dye from aqueous solution using yeast-treated peat as adsorbent: thermodynamics, kinetics, and equilibrium studies. Environ Earth Sci 75:357. https://doi.org/10.1007/s12665-016-5255-8